THE UNIVERSITY OF MICHIGAN
College of Engineering
Department of Mechanical Engineering
Cavitation and Multiphase Flow Laboratory

Report No. 01357-5-I

VIBRATION INDUCED CAVITATION OF A TURBULENT THRUST BEARING

(Submitted for Presentation and Publication to ASME)

by: W.K. Jekat
F.G. Hammitt

Financial Support Provided by:
National Science Foundation
Grant No. GK-1889

July 1969

ABSTRACT

Cavitation damage in a water-lubricated thrust bearing under conditions wherein the time-mean pressures do not indicate

ACKNOWLEDGMENTS

The experimental work herein reported was accomplished at and financed by the Worthington Corp., Harrison, N. J. Some of the analysis and the preparation of the manuscript was supported at the University of Michigan, Mechanical Engineering Department by National Science Foundation Grant No. GK-1889.

TABLE OF CONTENTS

LIST OF ILLUSTRATIONS

I. INTRODUCTION

Cavitation in journal and thrust bearings under steady-flow conditions is possible and has been studied for many years. Often this phenomenon results in relatively steady-state cavities or streamers of vapor or air. Theoretical analyses as well as excellent photographs of this flow regime have been recently published by Taylor [1]. Since the flow is steady and involves fixed cavities rather than growing and collapsing bubbles, it may not be a particularly damaging type of cavitation. Also, designers can avoid the condition with relative certainty since the calculation of the steady-state pressure distribution in a bearing is relatively well known.

Non-steady conditions, however, in high-speed flow machinery can easily induce highly damaging cavitation through a variety of mechanisms. Previous investigators concerned with studies of some of these mechanisms are Taylor [1], Endo [2], Hunt [3], and Frossel [4]. The examination of some of these mechanisms, with special reference to a water-lubricated thrust bearing in which cavitation occurred and was damaging, is the subject of this paper. In this particular case, steady-state calculations and measurements did not indicate the possibility of cavitation occurring.

II. DESCRIPTION OF TESTED BEARING AND TEST SET-UP

The tested bearing is a water lubricated fixed wedge thrust bearing made from SAE 660 bronze. It has eight pads, one of which is shown in Fig. 1. The test speed is 40,000 RPM which is produced by a small air turbine (Fig. 2). Air pressure on a loading piston imposes a constant load of 250 lbs. on the thrust bearing.

The film thickness is measured with a 1/4 inch diameter inductance coil transducer imbedded in the flat portion of the bearing together with a Model 3851-B amplifier* and displayed on a standard oscilloscope. For the test load the mean film thickness is 1.2 mil. During each revolution the film thickness varies from a maximum of 1.5 mil to a minimum of 1.0 mil. The movement is sinusoidal and is caused by conical rotor unbalance and thrust collar run-out. During the test this axial vibration was observed to be constant in regard to amplitude and frequency.

Seven pressure tap holes were drilled at a radius of 1.32 inches. Each of the holes was connected to a high precision bourdon-type pressure gage.

Water of $150^{o}F \pm 5^{o}F$ was supplied to the lubricating grooves in front of the bearing wedges. The pressure in the lubricating groove was 72 psig. The pressure around each individual bearing pad was atmospheric.

---

*Both items supplied by Electro Products Laboratory

III. TEST RESULTS

The measured pressures at the bearing surface are given in Fig. 3. They are mean pressures since the pressure gages cannot follow the high frequency (666 cps) pressure variations which must exist due to the cyclical change of film thickness.

The bearing was first inspected after 600 million revolutions (250 hours) and slight cavitation damage was noted. Testing was resumed until a total of 1080 million revolutions (450 hours) was accummulated. After this period the cavitation pitting was sufficient to detect a clear geometrical pattern.

The cavitation damage is typical, manifesting itself as a roughness of the surface which is apparently produced by numerous small overlapping pits. It covers all flat portions of the bearings as well as the end, i.e. the more raised portion, of the wedge. The beginning of the wedge – which is 2.5 mils below the flats – is free from damage.

IV. POSSIBLE MECHANISMS PRODUCING CAVITATION

The measurements of the time mean pressures within the bearing (Fig. 3) do not reveal any values below the vapor pressure. Therefore, the cavitation damage is obviously not caused by steady-state conditions in this case.

We thus turn to pressure fluctuations caused by the vibratory movement of the thrust collar as the possible mechanism cuasing vibration damage. Such pressure fluctuations can be considered as produced by two processes: 1) Squeeze film effects and 2) generation of acoustic pressure waves. The effects of these two mechanisms are of course additive. They are considered in more detail in the following sections. The first mechanism is based on friction effects and its analysis neglects inertial effects, whereas the second mechanism is analysed, neglecting friction, but considering inertial effects in a compressible liquid. A more exact, but prohibitively complex analysis would be obtained if frictional and inertial effects were considered together in a compressible fluid.

A. Derivation of Laminar Squeeze Film Pressure Distribution

The distance between the thrust plate and the bearing surface changes cyclically. During the "up-stroke", when the distance is increasing, fluid from the surrounding area flows into the increasing gap. This flow is induced by a reduced pressure within the gap. During the "down-stroke", when the distance decreases, the pressure in the gap is increased and fluid passes out of the clearance gap.

The process can be likened to a positive displacement pump. The displacement is:

$$-Q = VF \qquad \text{- - - (1)}$$

V is the velocity of approach and F the total pad area. Any depressions in the bearing surface have the character of dead spaces and do not alter the displacement so long as the pressures are low enough so that the compressibility of the fluid can be neglected.

The fluid flowing out of or into the gap encounters resistance. Therefore, the pressure will drop in the flow direction. For laminar flow over a land of the width b and with a flow path of length, ℓ (see Fig. 4), we have the well-known relations:

$$q = \frac{(P_1 - P_2)h^3}{12\,\mu} \frac{b}{\ell} \qquad \text{- - - (2)}$$

The bearing pads under investigation have four lands of different widths and flow paths lengths. Therefore, we consider the flows over the individual lands separately (see Fig. 1):

$$q_1 = \frac{(P_1 - P_2)b_1 h^3}{12\,\mu \ell_1}$$

$$q_2 = \frac{(P_1 - P_2)b_2 h^3}{12\mu \ell_2} \qquad \text{- - - (3)}$$

$$q_3 = \frac{(P_1 - P_2)b_3 h^3}{12\,\mu \ell_3}$$

$$q_4 = \frac{(P_1 - P_2)b_4 h^3}{12\,\mu \ell_4}$$

Summed, they must equal the displacement

$$Q = q_1 + q_2 + q_3 + q_4 \qquad - - - (4)$$

To estimate the effective width and mean flow path length for the individual lands, at least an approximate streamline pattern is required. This can be obtained graphically or by utilizing a flow analogy such as that provided by the electric analog field plotter. In the present case, the graphical procedure is very simple since three of the four lands are relatively narrow. In Fig. 1 the approximate boundary streamlines separating the lands are shown.

The center of the pad is occupied by a shallow inclined depression and a deep lubricant feed groove (Fig. 5). The maximum wedge depth is about twice the mean film thickness. To simplify the derivation the inclined depression and the feed groove are assumed replaced by one depression of constant depth, as shown by the dotted contours in Fig. 5. This depth is assumed to be large enough to make the pressure constant over the whole depression.

The foregoing assumption is based upon the fact that even a small depression goes a long way towards equalizing the pressure since the pressure drop is inversely proportional to the third power of the clearance, e.g. (5).

To roughly consider the squeeze film pressures at the beginning of the inclination, i.e., that portion of the inclined plane where the gap is the smallest, the length of the flat portion of pad 1 in the present example will be assumed increased somewhat beyond its actual length. Based on simple numerical estimates, a length increase of about one third (37%) has been assumed. The contribution of the wedge portion to the squeeze film pressure becomes very small at larger gaps because the squeeze film pressure is inversely proportional to the third power of the gap (see the following eq. 5). A more accurate

approximation than made here could be had by spetwise integration preferably on a computer.

We proceed now to derive the squeeze film pressure P_1 in the depression by substituting eq. (1) and (3) into (4)

$$P_1 = \frac{-12\,\mu\,VF}{h^3}\left(\frac{b_1}{\ell_1} + \frac{b_2}{\ell_2} + \frac{b_3}{\ell_3} + \frac{b_4}{\ell_4}\right)^{-1}$$

$$= \frac{-12\,\mu\,VF}{h^3 G} \qquad \text{- - - - (5)}$$

and $$G = \sum \frac{b_n}{\ell_n}$$

G is a geometry factor describing the land configurations.

The pressure P_2 surrounding the pad has been set equal to zero for convenience in this derivation. During the up stroke the sign of the velocity V is set to be negative and therefore the pressure P_1 in the depression becomes negative during this stroke and vice versa.

To study the likelihood of cavitation on the lands we must obtain the pressure distribution over them. We will, therefore, derive the pressure distribution over a streamline in the center of a land (Fig. 1). The flow path length x starts at the inner edge of the land. To determine the flow at x, i.e., q_x, and pressure on the land, one must exclude the displacement outside of the point x in order to find the flow at x:

$$q_x = q - \left[Vb\ell\left(1 - \frac{x}{\ell}\right)\right] \qquad \text{- - - (6)}$$

From the laminar flow law (2) we have

$$q_x = \frac{(P_1 - P_x)\, bh^3}{12\, \mu\, x} \qquad \text{- - - (7)}$$

Equating (6) and (7) and substituting eq. (2) for q yields the pressure distribution over any land

$$P_x = P_1\left(1 - \frac{x}{\ell}\right) - \frac{12\,\mu}{h^3}\, V\ell^2 \left(\frac{x}{\ell} - \frac{x^2}{\ell^2}\right) \qquad \text{- - -(8)}$$

The first term describes a linear pressure distribution over the land. The second term reaches a maximum at the middle of the land. This is due to the squeeze film effect on the land proper.

The film thickness h and the approach velocity V of the thrust collar normal to the surface vary cyclically in a vibrating bearing. We assume sinusoidal motion (Fig. 6) and set

$$h = h_m + A \sin(2\pi ft)$$

$$V = \frac{dh}{dt} = 2\pi fA \cos(2\pi ft)$$

Equations (5) and (8) for the sqeeze film pressure can now be rewritten as

$$P_1 = -24\pi\mu \frac{FA}{Gh_m^3} f \frac{\cos(2\pi ft)}{\left[1 + \frac{A}{h_m} \sin(2\pi ft)\right]^3} \qquad \text{- - - (11)}$$

$$P_x = P_1\left(1 - \frac{x}{\ell}\right) - 24\,\pi\mu \frac{A\ell^2}{h_m^3} f \frac{\cos(2\pi ft)}{\left[1 + \frac{A}{h_m} \sin(2\pi ft)\right]^3} \left(\frac{x}{\ell} - \frac{x^2}{\ell^2}\right)$$

$$\text{- - - (12)}$$

Investigation of (11) and (12) reveals that the maximum positive and negative pressures occur at a film thickness h which is smaller than the mean film thickness h_m [3] (see Fig. 6). It would therefore not be correct to set $\sin(2\pi ft) = 0$ and $\cos(2\pi ft) = -1$ to obtain these maxima.

Rather, we will find the pressure maxima when the expression

$$\frac{\cos(2\pi ft)}{\left[1 + \frac{A}{h_m}\sin(2\pi ft)\right]^3} = C_A \qquad \text{- - - (13)}$$

reaches its extreme values, as shown by consideration of eq. (11) and (12).

These extrema occur when

$$\frac{-\sin(2\pi ft)}{3\cos^2(2\pi ft)} = \frac{A}{h_m} . \qquad \text{- - - (13A)}$$

Therefore for every ratio of the amplitude to mean film thickness A/h_m there is a particular film thickness at which the squeeze film pressure reaches its positive and negative maxima, and this occurs at a point in the stroke which also depends on A/h_m. Thus Fig. 6 shows only a typical condition.

Fig. 7 gives the maximum value of

$$\frac{\cos(2\pi ft)}{\left[1 + \frac{A}{h_m}\sin(2\pi ft)\right]^3} = C_{A\text{-max}} \quad \text{versus} \quad \frac{A}{h_m} .$$

It is always larger than one, and increases rapidly with increasing A/h_m.

In our investigation we are mainly interested in the extreme pressures, particularly the negative extreme:

$$P_{1\text{-max}} = -24\,\mu\frac{\pi F A}{G h_m^3}\,C_{A\text{-max}}\,f \qquad \text{- - -(14)}$$

$$P_{x\text{-max}} = P_{1\text{-max}}\left(1-\frac{x}{\ell}\right) - 24\,\mu\pi\,\frac{A\ell^2}{h_m^3}\,C_{A\text{-max}}\,f\left(\frac{x}{\ell}-\frac{x^2}{\ell^2}\right) \qquad \text{- - -(15)}$$

The derivation has so far been made for laminar flow. The tested thrust bearing operated at a Reynolds Number

$$Re = \frac{U h_m}{\nu} = \frac{5520 \times 1.2 \times 10^{-3}}{6.75 \times 10^{-4}} \cong 10{,}000 \qquad \text{- - - (16)}$$

which is appreciably above the critical value of about 1000 [5]. Turbulent flow must, therefore, be expected. This was borne out by the observation that the load carrying capacity was about eight times larger than that predicted for laminar flow.

Turbulence will now be considered with the assumption that it is isotropic, i.e., the degree of turbulence is the same for all directions of flow in the bearing gap. The surface velocity U will be used to calculate the Reynolds number (and consequently the friction) so long as U is larger than any other velocity in the gap.

Turbulent Amplification Factor

Following [6] it has become customary to express the larger friction of a turbulent bearing by the ratio of turbulent to laminar friction factor. This ratio shall here be called the turbulent amplification factor T.

$$T = \frac{\text{turbulent friction coefficient}}{\text{laminar friction coefficient}} \qquad \text{- - - (17)}$$

If this ratio is known, then eq. (14) and (15) which are based on laminar flow could be corrected for turbulent flow.

The turbulent amplification factor is also the ratio of the wall shear stresses

$$T = \frac{\tau_{turb}}{\tau_{lam}} \qquad \text{- - - (18)}$$

For laminar flow we have Newton's expression

$$\tau_{lam} = \mu \frac{U}{h_m} \qquad \text{- - - (19)}$$

For the turbulent wall shear stress Prandtl [7] finds on the basis of empirical pipe friction data by Blasius

$$\tau_{turb} = 0.0225 \rho u^{7/4} \left(\frac{\nu}{y}\right)^{1/4} \qquad \text{- - - (20)}$$

The velocity u in the center of a pipe corresponds to U/2 in the center of the bearing gap:

$$u = \frac{U}{2} \qquad \text{- - - (21)}$$

$$y = \frac{h_m}{2} \qquad \text{- - - (22)}$$

Introducing eq. (19), (20), (21), and (22) into (18) we find for the turbulent amplification factor

$$T = 0.008 \left(\frac{U h_m}{\nu}\right)^{0.75} = 0.008 \, Re^{0.75} \qquad \text{- - - (23)}$$

For the conditions of our test the amplification factor becomes

$$T = 0.008 \, (10,000)^{0.75} = 8.0$$

Turbulent Squeeze Film Pressures

Eq. (14) and (15) for the pressure distribution over the bearing pad can now be rewritten for turbulent flow

$$P_{1\text{-max}} = -24\,\pi\,T\,\mu\,\frac{FA}{Gh_m^3}\,C_{A\text{-max}}\,f \quad ----(24)$$

$$P_{x\text{-max}} = P_{1\text{-max}}\,(1 - \frac{x}{l}) - 24\,\pi T\mu\,\frac{Al^2}{h_m^3}\,C_{A\text{-max}}\,f\left(\frac{x}{l} - \frac{x^2}{l^2}\right)$$

$$---(25)$$

These are the equations which we will now use to calculate the theoretical squeeze film pressure distribution over the tested bearing.

Calculation of Turbulent Squeeze Film Pressures

With the bearing configuration of Fig. 1

$f = 666\ \text{sec}^{-1}$

$A = 0.2 \times 10^{-3}$ inch

$h_m = 1.2 \times 10^{-3}$ inch

$\mu = 0.63 \times 10^{-7}\ \frac{\text{lb sec}}{\text{in}^2}$ (water at 150°F)

$P_v = 1.8$ psia

$F = 0.437\ \text{in}^2$

$G = 20.2$

$T = 8.0$

The maximum squeeze pressure in the depression can now be calculated. From Fig. 7 we obtain

$$C_{A\text{-max}} = 1.127$$

$$\text{for } \frac{A}{h_m} = \frac{0.2 \times 10^{-3}}{1.2 \times 10^{-3}} = 0.166$$

and then from eq. (24)

$$P_{1\text{-max}} = \mp 72.4 \text{ psi}$$

The pressure distribution over the wide land 1 ($\ell_1 = 0.42$ inch) is then calculated from equation (25):

$$P_{x\text{-max}} = \mp 72.4 \left(1 - \frac{x}{\ell_1}\right) \pm 583 \left(\frac{x}{\ell_1} - \frac{x^2}{\ell_1^2}\right)$$

Over the narrow land 3 ($\ell_3 = 0.07$ inch) we obtain

$$P_{x\text{-max}} = \mp 72.4 \left(1 - \frac{x}{\ell_3}\right) \pm 16.2 \left(\frac{x}{\ell_3} - \frac{x^2}{\ell_3^2}\right)$$

The calculated squeeze pressure distribution over the length of the pad is plotted in the upper portion of Fig. 3. Only the extreme pressures are given. The positive values occur during the down-stroke and the negative ones during the up-stroke. We are mainly interested in the negative pressures since they may be able to lower the bearing film pressures below the vapor pressure thus providing the possibility of cavitation. The largest negative squeeze pressure occurs roughly in the middle of the wide land and is -183 psia.

The subsequent analysis is considerably helped by measurements of the time averaged mean film pressures P_m. As previously explained, these were obtained by means of precision pressure gages connected to eight holes drilled into the bearing surface on the mean radius. The measured pressures are given as the central curve of Fig. 3.

The calculated squeeze film pressures have been added to and subtracted from the measured mean pressures. The results are the extremes of the transient pressure swings (Fig. 3).

The resultant minimum pressures are near the ambient pressure over much of the bearing pad and are below the vapor pressure on part

of the wide land. This, then, explains satisfactorily the cavitation damage in this region; even without assistance from the acoustic pressure oscillations discussed in the next section. On the narrow land, (not shown in Fig. 3) the minimum pressures come within 10 psi of the vapor pressure. Realizing that modifications of the assumed calculation model can easily change the results by 10 psi, we conclude that the identical damage to the narrow land is also caused by cavitation.

Once cavitation occurs, evaporation of the lubricant increases the flow resistance by blocking part of the active passage, similar to the effect in flashing labyrinth seals [8]. As a consequence, the pressure swings become larger. The pressures on the narrow land approach the vapor pressure and the cavitating zone on the wide land becomes larger.

B. Acoustic Pressure Oscillations

If an infinite flat plate immersed in a fluid oscillates through a small amplitude, high frequency stroke, the resultant fluid behavior is given to a first order by the "acoustic approximation" which neglects the velocity itself in comparison to the velocity derivatives. Though well-known [9, e.g.], the essentials of the derivation are repeated here for convenience. With this approximation, the one-dimensional Euler's equation becomes:

$$\frac{\partial v}{\partial t} = \frac{-1}{\rho} \frac{\partial P_1}{\partial x} \qquad \text{- - - (26)}$$

A velocity potential is then assumed for the resultant motion. Substituting into eq. (26), which is then integrated in x:

$$\frac{\partial \phi}{\partial t} = -P_1 \qquad \text{- - - (27)}$$

From this, the pressure as a function of time can be computed if the potential for the oscillatory motion is known. This is an easy matter if a simple harmonic motion is assumed, in which case $\phi = A \times \sin wt$ and the acoustic pressure, with respect to a zero datum, is given by:

$$P_1 = -\rho\omega\, cA \left[\cos(kx - \omega t)\right] \qquad - - - (28)$$

where $k = \omega/c = 2\pi f/c$

A = oscillatory half amplitude

c = sonic velocity of the fluid

The maximum oscillatory pressure differential from eq. (28) is clearly:

$$P_1 = 2\pi\rho fc\, A \qquad - - - (29)$$

Eq. (29) is in the form of the so-called "water hammer equation".

In the case of the thrust bearing under consideration, the oscillation is of course in the direction across the narrow gap rather than in a free space as assumed in the analysis. While the actual geometrical situation is too complex for easy analysis, it is certain that the pressure oscillations generated by the harmonic motion in this confined space through the mechanism here under consideration will be considerably greater than for the simplified case analysed, since the acceleration of the fluid parallel to the face necessary to accommodate the vertical harmonic motion will be much greater than those normal to it. Nevertheless an estimate will now be made for the acoustic pressure oscillation magnitude, if the vibration were in an open space, for the same conditions already considered for the squeeze film effect.

Let us assume the following applicable parameters as used for the squeeze film analysis:

$$f = 666 \text{ sec}^{-1}$$

$$A = 0.2 \times 10^{-3} \text{ inch}$$

In addition, assume the sonic velocity of water to be 4500 ft/ sec, and the density of water to be 62.4 lb m/ft^3. Then from eq. (29):

$$P_1 = 2\pi \rho fcA = \frac{2\pi \times 62.4 \times 666 \times 4500 \times 0.2 \times 10^{-3}}{32.2 \times 12 \times 144} = 4.2 \text{ psi},$$

whereas the squeeze film pressure differential for the same case was 183 psi. Hence in this case the acoustic pressure contribution is probably negligible.

For the acoustic mechanism as here analysed, the pressure oscillation is not a function of film thickness, or of pad contour. Hence this mechanism provides no important further explanation, beyond the squeeze film mechanism, for damage on those areas which have small film thickness. However, the opposite (unloaded) thrust bearing for the machine under consideration has 29 mils mean film thickness so that the squeeze film effect becomes negligible. Examination of the surface shows several regions of surface discoloration, mainly in the center of the pad. This mild attack would be consistent with acoustically induced cavitation wherein the pressure oscillations could be several times that estimated above, due to the effect of the confined geometry. In such a case instantaneous pressures below vapor pressure are a possibility on the unloaded bearing.

We thus have two cavitation damage mechanisms - one which is relatively strong, and one which is relatively weak for the present configuration.

C. General Comparison of Squeeze-Film and Acoustic Pressure Oscillation Magnitudes

The maximum pressure oscillation from the squeeze film effect is given by eq. (24) and that for the acoustic pressure oscillation (neglecting the amplifying effect of the actual restricted geometry) by eq. (29). A simple ratio between the P_1 values computed for either mechanism gives:

$$\frac{P_{1\,squeeze}}{P_{1\,acoustic}} \propto \frac{F C_{A\text{-}max} \sqrt{T}}{h_m^3 C} \qquad \text{- - - (30)}$$

where all symbols have been previously defined. $C_{A_{max}}$ is a complicated function of A/h_m as shown by eq. (13) and (13 A). Hence it will be assumed constant at a typical value as calculated for the present case. Then for a particular bearing configuration and fluid condition:

$$\frac{P_{1\,squeeze}}{P_{1\,acoustic}} \propto \frac{1}{h_m^3} \qquad \text{- - - (31)}$$

and does not depend on either amplitude or frequency, but is extremely sensitive to h_m with the squeeze-film effect becoming predominent for small h_m.

For the present bearing it was previously shown that

$$\frac{P_{1\,squeeze}}{P_{1\,acoustic}} = \frac{183}{4.2} = 43.5$$

If these effects were to become of the same order of magnitude it would be necessary that h_m be increased by a factor of $(43.5)^{1/3} \simeq 3.5$. Since the present $h_m = 1.2 \times 10^{-3}$, the squeeze-film effect in the present bearing would be reduced to the same order as the acoustic effect if the mean clearance were increased to about 4 mils. Hence, it is not a safe general assumption that the acoustic effect can be neglected.

V. OTHER POSSIBLE CONTRIBUTORY EFFECTS AND GENERAL CONSIDERATIONS

A. Surface Discontinuity and Entrance Effects

The peripheral velocity of the present bearing is about 11,000 ft/min. The kinetic fluid pressure corresponding to this is about 225 psi. It is reasonable to assume that the fluid adjacent to the moving surface will have approximately the velocity of the surface, and hence this may be approximately the fluid velocity approaching the narrow portion of the gap (Fig. 5). Any discontinuity in this turbulent flow region such as a sharp corner at entrance or a bump might easily have a pressure coefficient of the order of 0.2 [10], which could then cause a local pressure drop of 0.2 x 225 = 45 psi. Such a local drop would obviously be a strong contributory factor toward cavitation nucleation under the existing pressure distributions (previously discussed) or might well be sufficient in itself in certain regions (Fig. 3) to cause cavitation.

If it is assumed that the effective fluid velocity is about 1/2 the peripheral bearing velocity as would be anticipated to be the case for full-developed flow within the narrow part of the gap, the kinetic pressure would be reduced by a factor of 4 so that a surface discontinuity with an 0.2 pressure coefficient would produce a local pressure drop of only about 11 psi. This too would, however, be then a non-negligible effect. The effects of surface roughness on cavitation in a flow over stationary objects has previously been considered in some detail by Holl [11] with results consistent with the above discussion.

B. Venturi Effects

Any local configuration giving a pressure recovery factor of 0.5 (a very poor diffuser efficiency) would allow a local pressure reduction of 50% of the kinetic pressure, i.e. about 28 psi if it is assumed that the fluid velocity is $\sim 1/2$ the bearing velocity and 112 psi if the full bearing velocity is used. It is conceivable that the required geometrical conditions could exist around the exit from the close gap region (Fig. 5) or around the outer periphery of the bearing (Fig. 1) if there is a slight rounding of corners or relief of the land near the exit. This effect could then be responsible for the cavitation pitting observed around the outside periphery of the bearing.

C. General Considerations

1. Nucleation and Damage Sites

Much of the previous discussion has emphasized the generation of low pressure regions wherein cavitation bubbles could be nucleated. However, it is not necessarily true that the damage will be limited to these regions or even occur within them. It has been assumed in the analysis that the driving frequency is that of the RPM (40,000 rpm = 667 cycles/sec). If the fluid velocity in the bearing is 1/2 the bearing velocity and the bubbles are assumed to move with the fluid velocity, then a bubble nucleated during the low pressure portion of the cycle would move approximately 1/4 of the bearing circumference before collapsing in the next high pressure portion of the cycle. Hence it is easily conceivable that bubbles nucleated at any

spot within the bearing could migrate to any other position on one of the 8 pads before collapsing. Thus is appears likely that bubbles will nucleate predominently at minimum pressure regions (see Fig. 3) but that damage is likely to be most severe in high pressure regions where the collapse violence will be greatest. A consideration of the damage locations bears out this general conclusion.

2. Damage as Affected by Operating Conditions

In general the bearing clearance is decreased as load is increased and the fluid pressures within the bearing are also increased. However, the predominent pressure oscillation, that due to the squeeze-film effect, increases with the inverse cube of clearance (eq. 24), which is a much greater effect than the increase in mean pressure mentioned above. Hence, cavitation nucleation becomes more likely for the loaded bearing even though the mean pressures therein are higher. Cavitation damage becomes still more likely under these conditions because of the increased bubble collapse pressure.

VI. CONCLUSIONS

The following are the major conclusions from this study.

1) Cavitation and cavitation damage can occur in a thrust bearing of relatively conventional design under conditions for which cavitation would not normally be anticipated from the time-mean fluid pressures.

2) Various mechanisms exist which are capable of causing transient under-pressures of sufficient magnitude to nucleate bubbles in the bearing considered. The most important of these is probably the squeeze-film effect generated by vibratory motion in the axial direction. The effect is greatly enhanced if the flow is turbulent as appears to be the case in the present instance.

3) Other important mechanisms are the effects of local surface discontinuities and the "acoustic pressures" generated by the axial vibratory motion. These latter are relatively un-important in the present instance but their relative importance increases very rapidly as the bearing clearance is increased.

4) The observed damage pattern can be fully explained on the basis of these various mechanisms.

REFERENCES

1. G. I. Taylor, "Cavitation in Hydrodynamic Lubrication", Cavitation in Real Liquids, Prac. of Symposium at General Motors Research Laboratories, Warren Michigan, 1962, edited by R. Davies, Elsevier Publishing Company, New York, 1964.

2. K. Endo, T. Okada, M. Nakashima, "A Study of Erosion between Two Parallel Surfaces Oscillating at Close Proximity in Liquids", ASME Paper No. 66-Lub-9, to be published Trans. ASME, J. Basic Engr.

3. J.B. Hunt, "Cavitation in Thin Films of Lubricant", The Engineer, Jan. 29, 1965, pp. 22-23. "Pressure Distribution in a Plane Fluid Film Subjected to Normal Sinusoidal Excitation", Nature, Vol. 211, No. 5054, pp. 1137-1139, September 10, 1966.

4. W. Frossel, "Schwingungskavitation in Gleitlagern".

5. S. Abramowitz, "Turbulence in a Tilting-Pad Thrust Bearing," Trans. ASME, Vol. 78, 1956, pp. 7-11.

6. E.B. Arwas, B. Sternlicht, and R.J. Wernick, "Analysis of Plain Cylindrical Journal Bearings in Turbulent Regime", MTI-62TR22, 1962.

7. L. Prandtl, "The Mechanics of Viscous Fluids," Aerodynamics Theory, W.F. Durand ed., Division G., Dover Publications, New York, N.Y., 1963, (originally published by J. Springer, 1935).

8. A. Agostinelli and V. Saleman, "Prediction of Flashing Water Flow through Fine Annular Clearances", Trans. ASME, Vol. 80, July 1958, pp. 1138-1142.

9. H. Lamb, Hydrodynamics, Dover Publications, New York.

10. J.W. Holl, "The Inception of Cavitation on Isolated Surface Irregularites," Trans. ASME J. Basic Engr., March 1960, pp. 169-183.

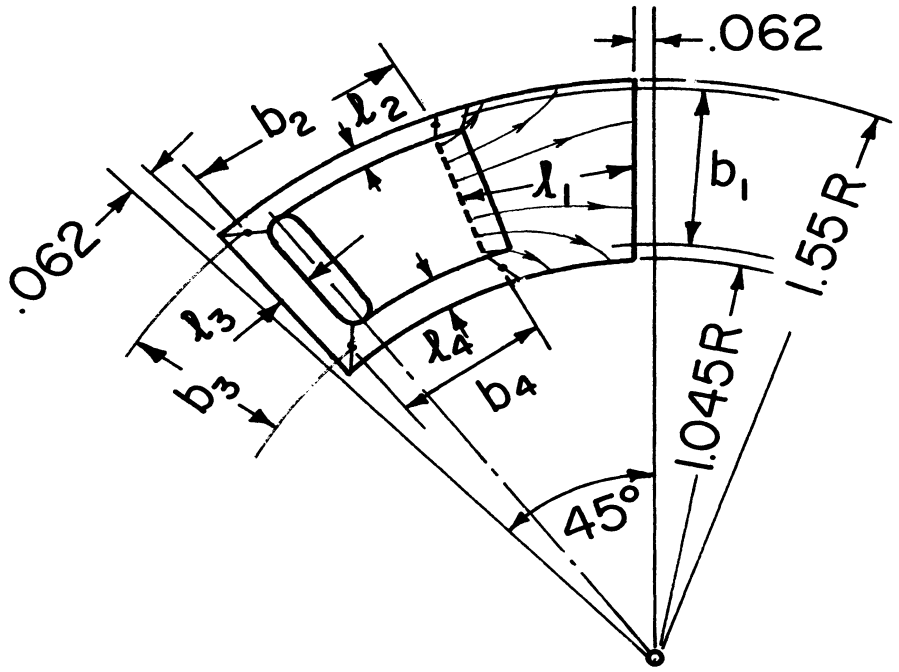

$b_1 = 0.43$ in ; $\ell_1 = 0.42$ in
$b_2 = 0.48$ in ; $\ell_2 = 0.05$ in
$b_3 = 0.43$ in ; $\ell_3 = 0.07$ in
$b_4 = 0.28$ in ; $\ell_4 = 0.08$ in

$G = 20.2$
(Equation 5A)

$$\frac{b_1}{\ell_1} + \frac{b_2}{\ell_2} + \frac{b_3}{\ell_3} + \frac{b_4}{\ell_4} = \frac{0.43}{0.42} + \frac{0.48}{0.05} + \frac{0.43}{0.07} + \frac{0.28}{0.08} =$$

$$= 1.02 + 9.6 + 6.1 + 3.5 = 20.2 = G$$

2909

Fig. 1. One Pad of the Test Bearing

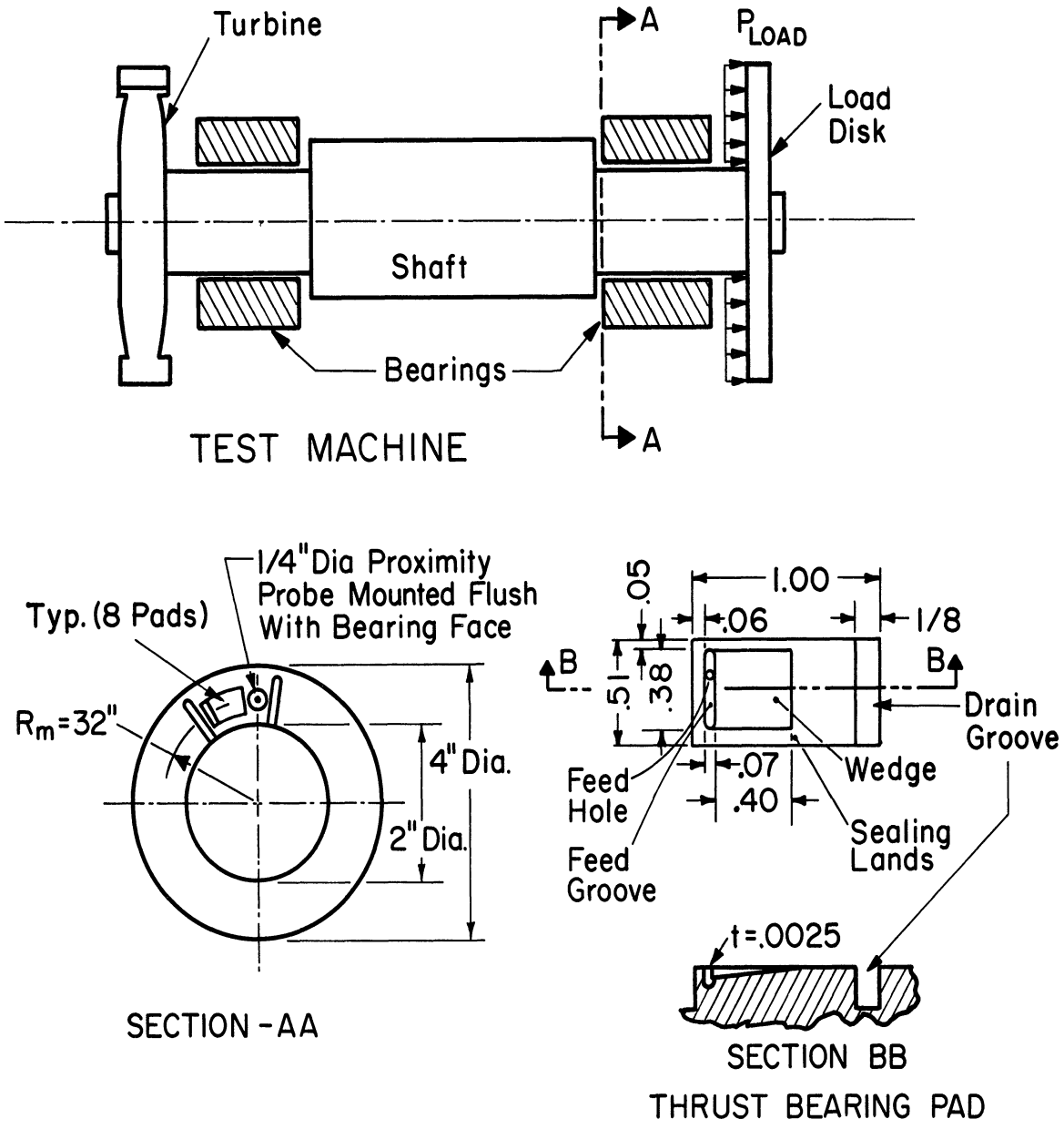

Fig. 2. Test Setup

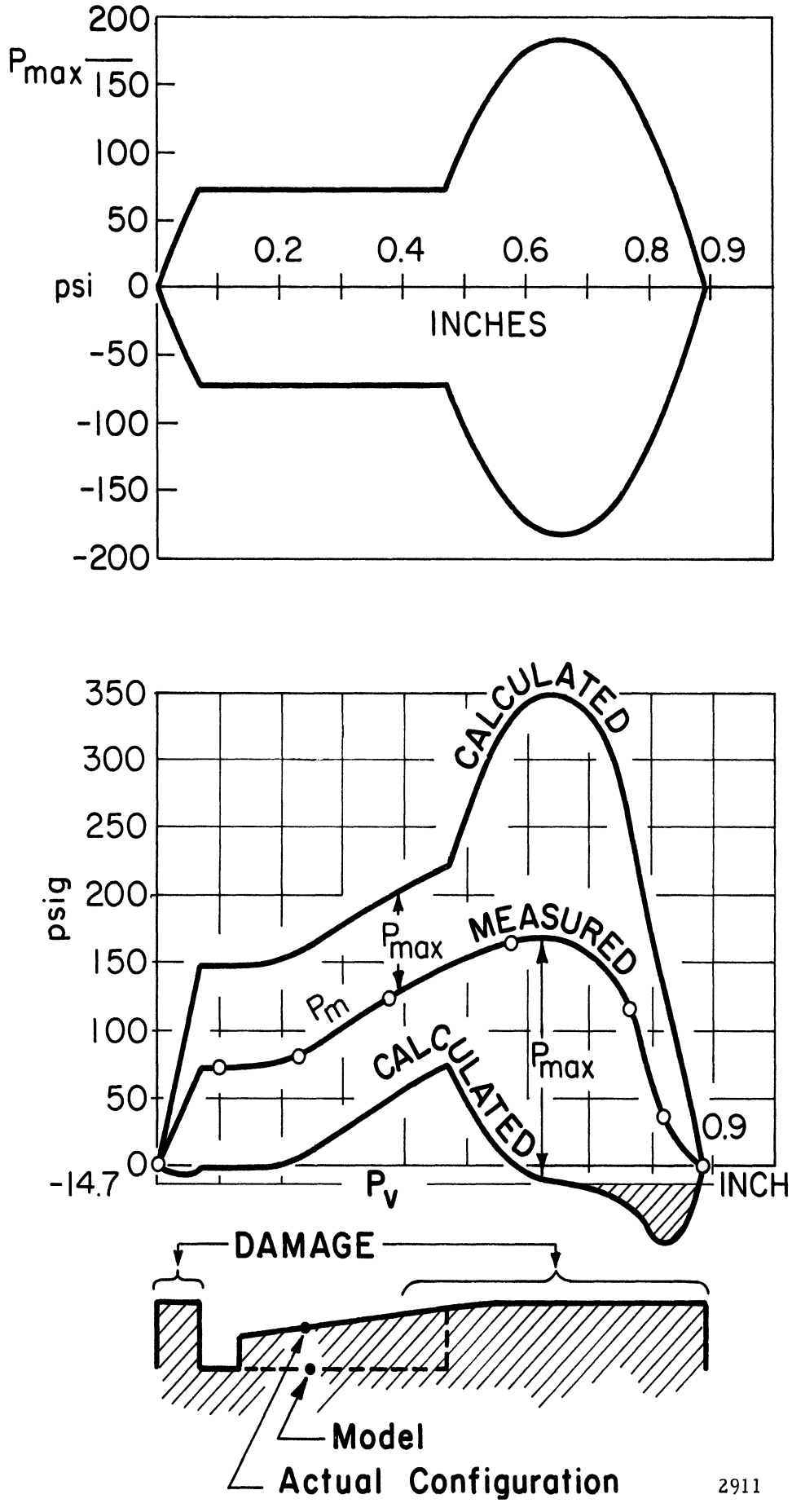

Fig. 3. Pressure Distribution

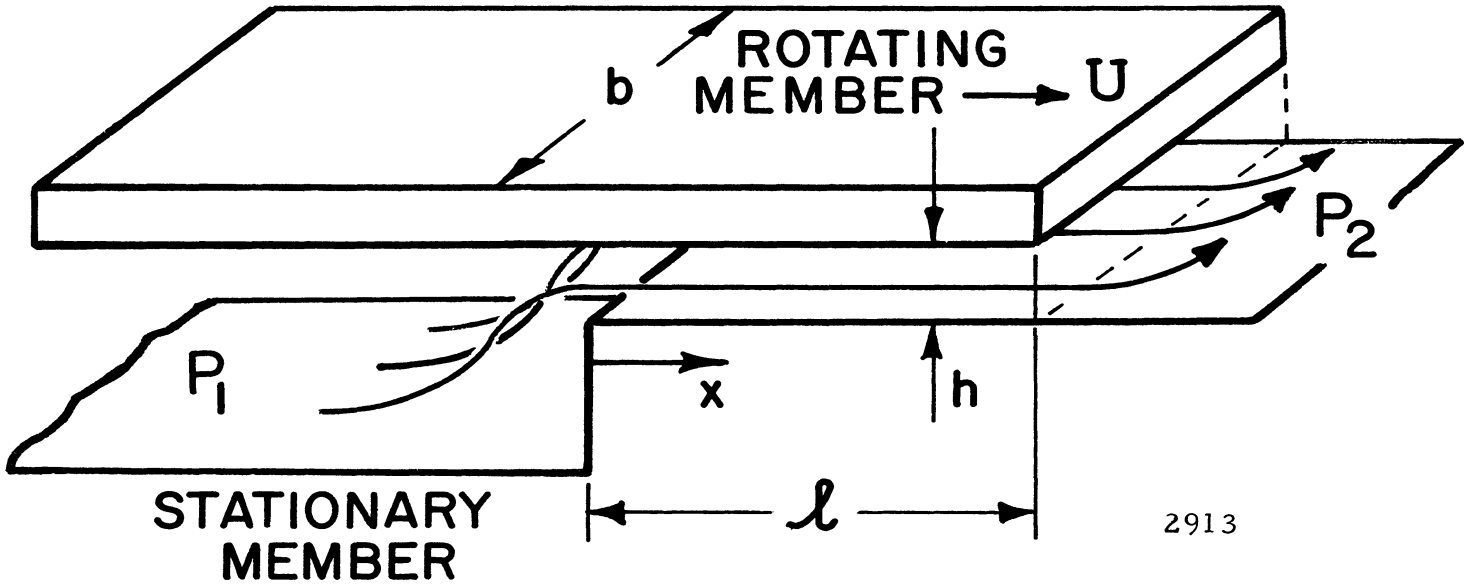

Fig. 4. Flow in Gap

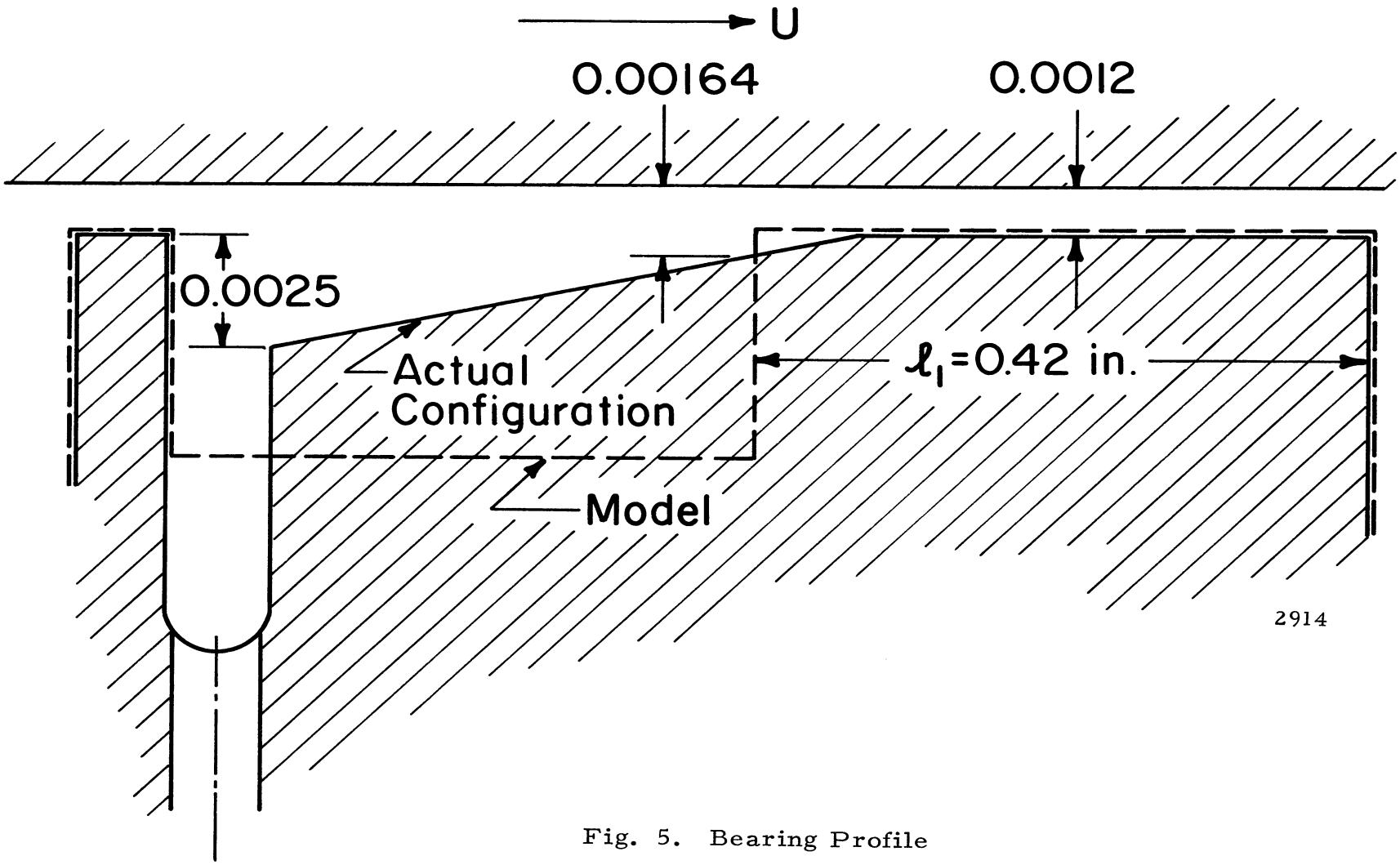

Fig. 5. Bearing Profile

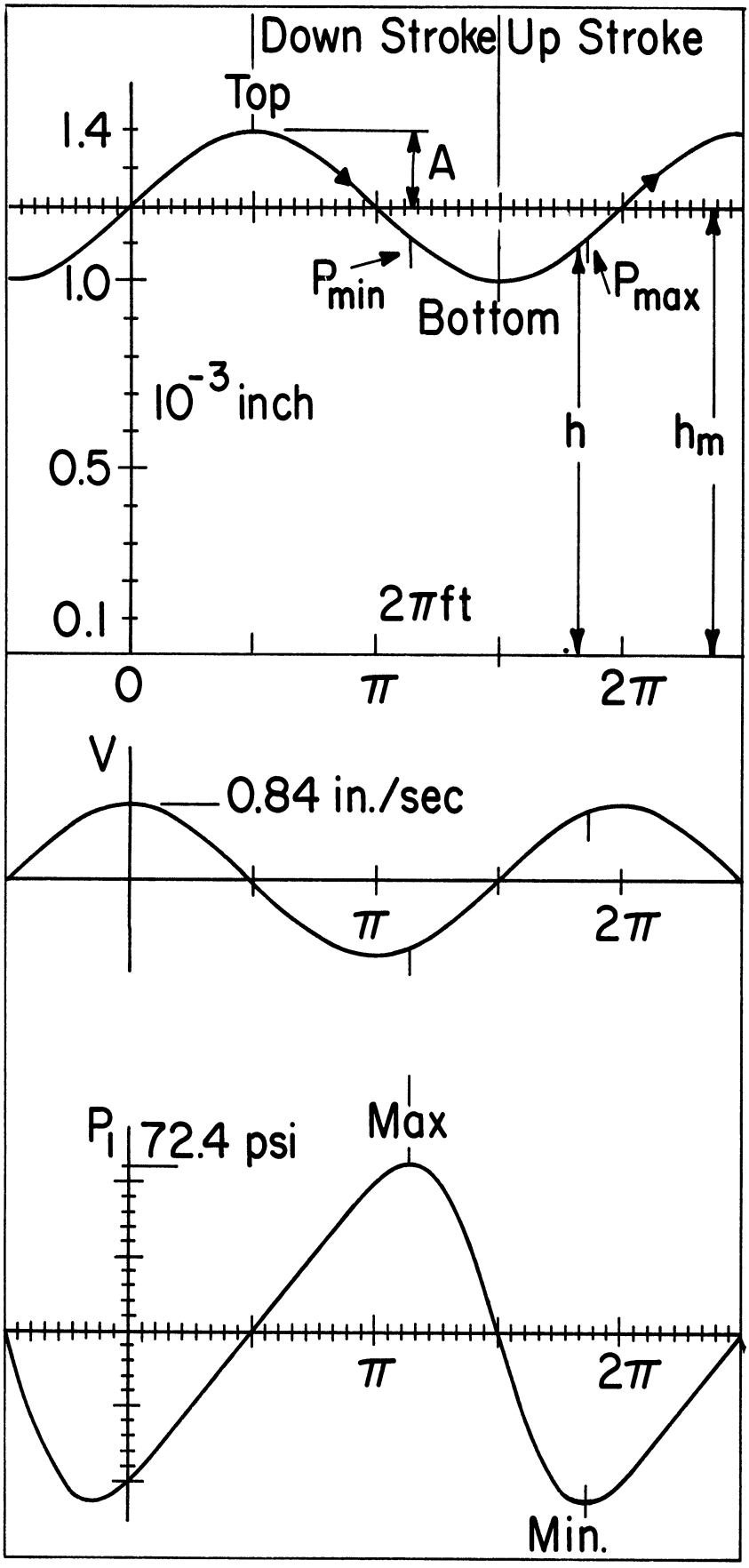

Fig. 6. Bearing Vibration

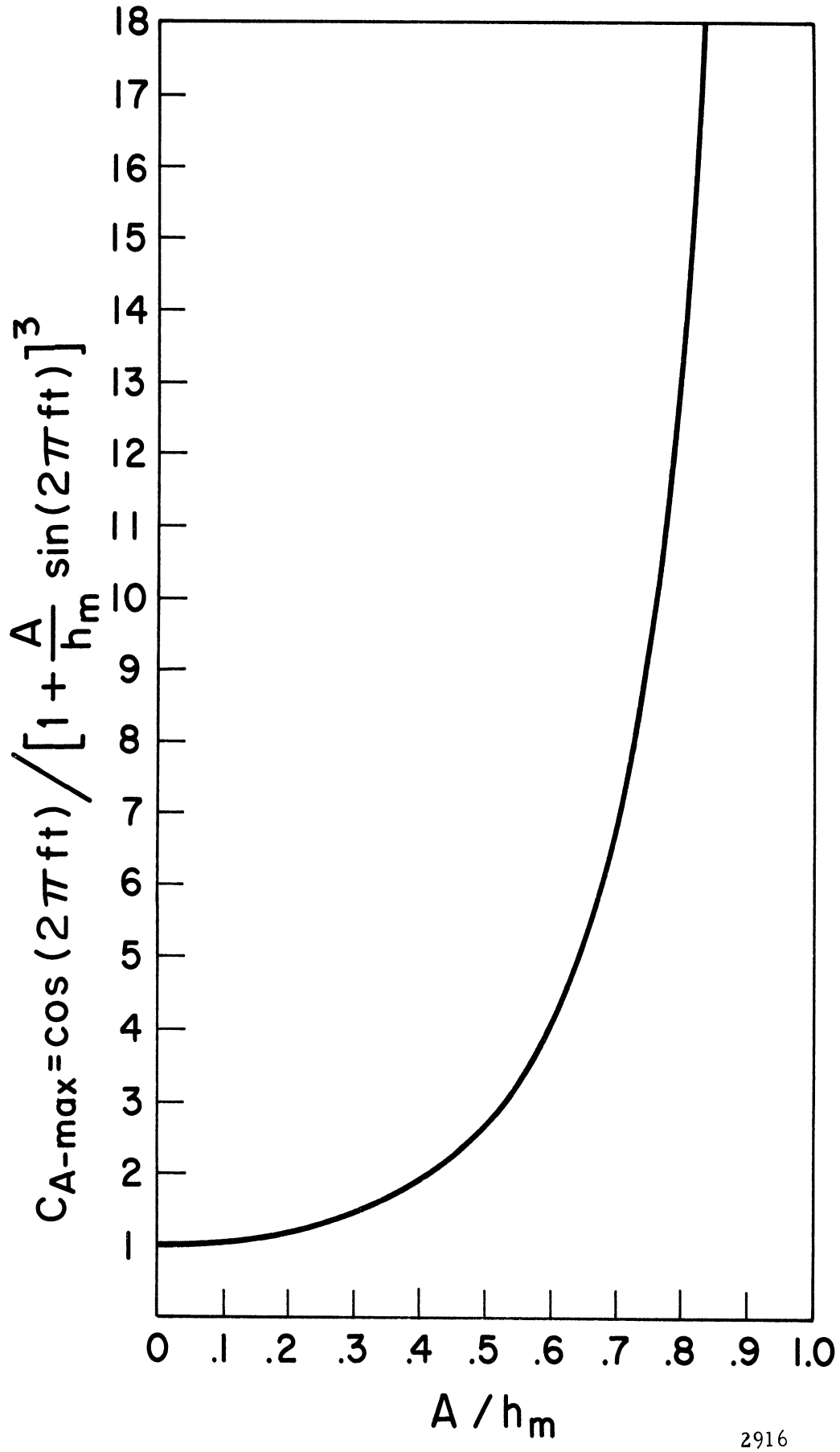

Fig. 7. $C_{A\text{-}max}$ versus A/h_m